Direct observation of remanent magnetic states in epitaxial fcc Co small disks

C. A. F. Vaz, L. Lopez-Diaz, M. Kläui, and J. A. C. Bland*

Cavendish Laboratory, University of Cambridge, Cambridge CB3 0HE, United Kingdom

T. L. Monchesky and J. Unguris

National Institute of Standards and Technology, 100 Bureau Drive Stop 8412, Gaithersburg, Maryland 20899-8412

Z. Cui

Rutherford Appleton Laboratory, Chilton, Didcot OX11 0QX, United Kingdom

The magnetic nanostructure of epitaxial fcc Co/Cu(001) circular elements ($\sim 1.7 \mu$m in diameter) has been imaged with scanning electron microscopy with polarization analysis. The disks are obtained by ultrahigh vacuum deposition of the metal films onto a prepatterned Si(001) substrate. The Si structures are 700 nm high, ensuring that the continuous background film and that of the circular structures are not physically connected. A closed flux configuration (a quadrant configuration) is observed for some of the disks, characteristic of systems with cubic anisotropy. The measured width of the 90° domain wall varies from 70 ± 25 nm close to the vortex core, up to 150 ± 25 nm at a normalized distance $r/r_d \approx 0.625$ from the vortex core (where r_d is the domain wall length from the vortex core to the disk periphery), i.e., significantly exceeding the bulk domain wall width, and increasing further with increasing distance from the vortex core. Such a wide domain wall is a consequence of the geometrical constraints imposed by the element, thus defining a geometrically constrained domain wall. This view is supported by detailed micromagnetic simulations that also show that the domain wall width increases dramatically with radial position from the disk center.

Small magnetic elements have received considerable attention recently in large measure due to their potential for memory elements in high-density storage media or as miniaturized sensor elements,[1] but also because they have opened a new field of research with its specific problems and dedicated experimental techniques. Of particular interest is the study of the equilibrium magnetic states and magnetization reversal mechanisms in small elements, which are strongly determined by the interplay of the different anisotropy terms with the physical shape of the element. In fact, the shape of the element so fundamentally influences the switching behavior of the magnetization that a large effort has been spent with the purpose of finding the geometry that provides the simplest, fastest, and most reproducible switching mechanism, which are essential prerequisites for device applications.[1–6] As a striking example of the influence of the shape in the equilibrium magnetic state, it is observed that micrometer sized NiFe circular elements show a circular magnetization state (vortex state),[7] while square elements show a domain state that resembles the Landau-Lifshitz (quadrant) domain structure.[8] In both cases, the magnetostatic energy is minimized by flux closure commensurate with the element geometry. No extra cost arrives from the anisotropy term, which in NiFe is negligible compared with the magnetostatic energy term, but for other materials the effect of the anisotropy is expected to play an important role in determining the equilibrium magnetic states and ultimately the reversal of the magnetization process. In fact, the role of the magnetic anisotropy has not been so extensively investigated, although some studies have used epitaxial systems such as fcc Co(001),[2,9] hcp Co(0001),[10] bcc Fe(001), and bcc Fe (110).[11] In general, the effect of the magnetic

anisotropy is to restrict the states with flux closure to those compatible with local domains pointing along the easy direction axis. In disks, materials with cubic anisotropy form quadrant structures, and materials with uniaxial anisotropy have a multidomain state with parallel magnetic domains.[11] Ring structures, in contrast, show local domainlike features when a cubic anisotropy is present.[12] Less clear, however, is how the magnetocrystalline anisotropy and the dipolar interactions (i.e., shape of the element) together determine the form and extent of the effective transition at a magnetic domain boundary in small elements. More generally, there is strong current interest in the concept of a geometrically constrained domain wall.[13,14]

In this paper, we use scanning electron microscopy with polarization analysis (SEMPA) to study the remanent states in micrometer size fcc Co(001) disks epitaxially grown on the Cu(001) surface. In particular, we look into the details of the domain wall between the observed magnetic domains to show that it is strongly constrained by both the shape of the element and the magnetic anisotropy. The SEMPA technique has the advantage of not influencing the magnetic state of the sample, unlike more invasive techniques such as magnetic force microscopy.[15] In addition, Co thin films deposited on the Cu(001) surface have been extensively studied[16–20] and provide a well characterized system, ideal for the study of magnetic elements.

The elements studied here were fabricated by deposition onto a prepatterned Si(001) substrate. A mask consisting of an array of disks and rings was first defined on the resist layer by electron-beam lithography and the unprotected Si was etched down by reactive ion etching. In this paper, we consider only the magnetic characterization of the disk
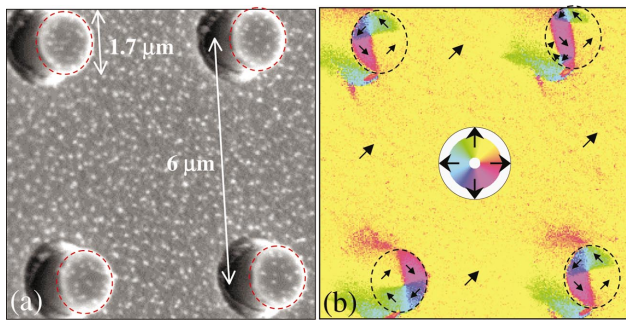
FIG. 1. (Color) SEMPA images of four disks: (a) topography of the disks showing the Si pillars rising well above the background (the bright spots have been identified as Au clusters remaining after the sputtering off of the capping layers and have negligible influence over the magnetic signal). (b) Magnetization direction. Because of the measurement geometry, the magnetization data just to the left of the disk is in the shadow of the detector and should be ignored. Superimposed circles and arrows are guides to the eye. The inset shows the key to the orientation of the magnetization.

elements.[12] The disk diameter was fixed at ~ 1.7 μm and the separation between the elements was set to 6 μm. This assures that the disks do not interact with each other. Before film deposition, the Si prepatterned substrate was etched in a 10% HF solution and loaded into the MBE chamber (base pressure $\sim 3 \times 10^{-10}$ mbar). A 100-nm-Cu(001)-template layer was first deposited onto the Si(001) substrate onto which a 34-nm-Co layer was deposited [Co grows epitaxially in the fcc phase on the Cu(001) surface[17]]. A thin 2-nm-Cu layer was then deposited and this trilayer was finally capped with a 4-nm-Au layer to prevent oxidation of the structure. The height of the Si structures (700 nm) is such that the continuous background film and that of the circular structures are not physically connected.[9] A top view scanning electron microscopy image of some of the disks is shown in Fig. 1(a). This method was previously shown to yield successful results for ring elements,[2,9,21] where a stable bidomain state was observed at remanence.

The magnetic domain structure of the elements was imaged at remanence with SEMPA.[22] The sample is introduced into a ultrahigh-vacuum chamber and the sample capping layers are sputtered off. A high-energy electron beam is fo-
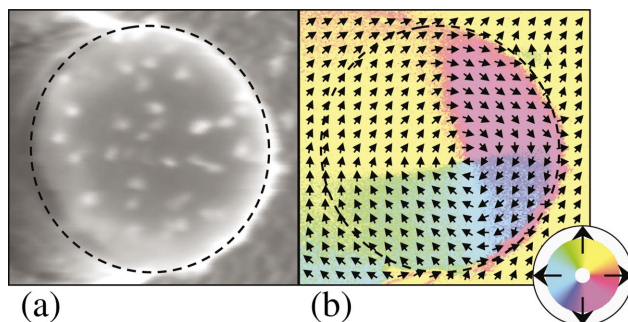

FIG. 2. (Color) SEMPA image of a disk with a quadrant state at higher magnification showing: (a) topography, and (b) magnetization direction. The magnetization direction is given both by color, keyed to the inset color wheel, and the superimposed arrow field.
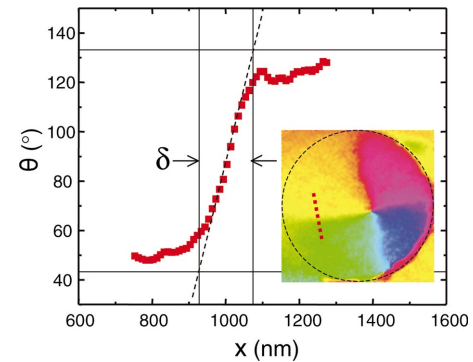

FIG. 3. (Color) Domain wall magnetization profile between two domains.

cused onto the sample surface and the intensity and spin polarization of the emitted secondary electrons are measured, enabling simultaneous imaging of the topography and the magnetization. Both orthogonal magnetization components within the plane of the sample are measured, so that the magnitude and direction of the in-plane magnetization are completely determined. The probing depth of the secondary electrons is limited to ≈ 1 nm, making this technique a sensitive surface magnetometer.

The SEMPA images for four of the disks (representative of the total of the disks imaged) are shown in Fig. 1. Three of the disks present a nearly closed flux, four-quadrant configuration typical of a system with cubic anisotropy. The magnetization inside each quadrant domain is oriented along one of the $\langle 110 \rangle$ directions, the easy magnetization axis of fcc Co(001). This is the prevalent state observed for the disks, but other magnetic configurations are also observed. In particular, the top right disk exhibits a magnetic state composed of two vortex cores with opposite circulations. As will be shown below, this can be understood in terms of the relaxation mechanism from saturation to remanence, where the two vortex cores become pinned, therefore inhibiting relaxation towards the equilibrium state. All of the disks have some net magnetic moment, since one of the domains is usually larger than the others (in particular, the vortex core does not sit exactly in the center of the disk). The magnetization direction in this domain is the same as in the background film and in the direction along which the field was applied.
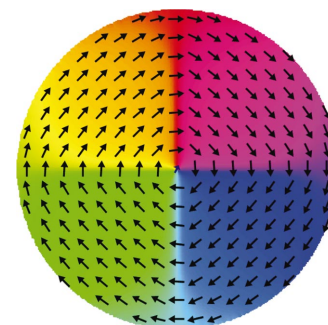

FIG. 4. (Color) Micromagnetic simulation for the remanent state after saturation.

A higher magnification image of one of the disks, shown in Fig. 2, allows a closer look into the details of the four-quadrant domain structure. In particular, an estimate of the width of the 90° domain wall can be obtained at this resolution. A domain wall profile between two domains is shown in Fig. 3. This line scan corresponds to the line drawn across the disk inset in the figure. We determine the domain wall (DW) width from the slope of the magnetization line scan at the middle of the domain wall $[\delta = (\pi/2)(\partial\theta/\partial x)_0^{-1}]$, as shown in Fig. 3. For this wall, the measured width is 150 ± 25 nm. This is much wider than the value expected in bulk or continuous film systems.

In order to understand both the remanent magnetic states observed and the width of the domain wall, we performed micromagnetic simulations to first calculate the equilibrium state at remanence (starting from the saturated state along the magnetocrystalline easy axis direction) and second, to model the dynamics of the domain formation. The micromagnetic simulations were based on the OOMMF micromagnetic package.[23] The Co parameters used were $M_s = 1.424 \times 10^6$ A/m for the saturation magnetization and $A = 3.3 \times 10^{-11}$ J/m for the exchange constant. The value of the anisotropy constant is crucial in determining the equilibrium state of the system. For fcc Co/Cu(001), the anisotropy constant has been estimated as $5 \pm 1 \times 10^4$ J/m^3,[18–20] not too dissimilar from the bulk value 6×10^4 J/m^3.[24] In our simulations, we used the experimental value[2] 6.5×10^4 J/m^3 and the thickness was set to 34 nm. The magnetization is assumed to be uniform in the vertical direction and a cell size of $(4 \text{ nm})^2$ is considered in the plane of the particle. For the present study, the magnetization was first saturated along one magnetic easy axis and then was allowed to relax under no applied field. The equilibrium state at remanence as obtained from the micromagnetic simulations is shown in Fig. 4.

The simulations show that, after saturation in an in-plane magnetic field, the dominant remanent equilibrium state is the quadrant state, as observed experimentally. The domain formation occurs by nucleation of two vortex cores on two opposite edges of the disk where the magnetostatic energy is maximum (i.e., at the ends of the dipole defined by the saturated state). The vortices need not occur simultaneously, and one may have a smaller nucleation energy and propagate throughout the disk, thus creating the quadrant state. When two vortices are created (as observed in our simulations), one of the vortices moves to the center of the disk and pushes the other outwards until it vanishes. In few instances, it may happen that these vortices are pinned by defects, and are still present in the remanent state as observed in some of the disks (top right disk of Fig. 1). As noted before, the disks imaged have a net magnetic moment. Two mechanisms may be responsible for this behavior; (i) due to the stray field that results from the cavity in the background film (dipolar interaction) and (ii) pinning of the vortex core at film defects during the magnetic relaxation process. An expression for the upper limit of the stray field along the film magnetization (y direction) at a height z above the center of the cavity (origin of the coordinate system) is readily calculated as $H_y(0,0,z) = \pi M_s t r_0^2/(z^2 + r_0^2)^{3/2}$ Oe for film thickness $t \ll r_0$, where M_s is the saturation magnetization and $r_0 = 0.85$ μm is the

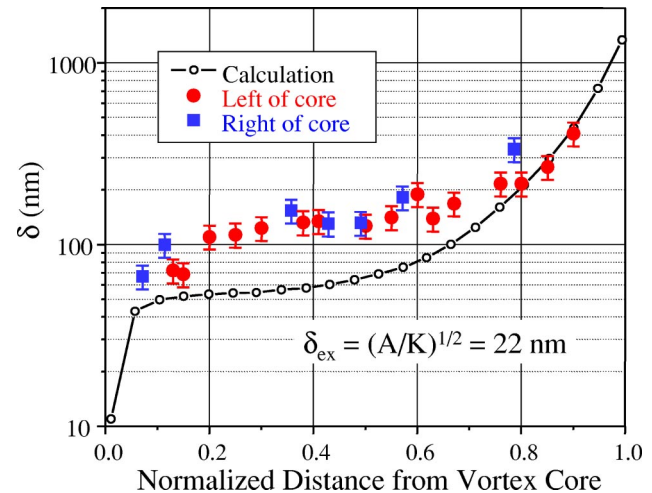radius of the cavity (disk). At a height of 0.7 μm, we obtain $H_y \approx 80$ Oe (at the center of the disk). This assumes a uniform magnetization throughout, while the magnetization will likely twist at the edges of the cavity in order to reduce the stray field. From micromagnetic simulations, we obtain a displacement of the vortex core with applied magnetic field of 3.7 nm/Oe, which would correspond to a displacement of 0.3 μm under a magnetic field of 80 Oe. The displacement observed for the disk shown in Fig. 2 is half of this value, 0.15 μm. If the displacement were due to the stray field only, its magnitude should be closer to 40 Oe. This value is, however, comparable to that corresponding to the strength of the pinning sites, which for a 34-nm-thick continuous Co film is of the order of 40–100 Oe (value of the coercive field along the easy axis direction), so that either or both effects could be responsible for the displacement of the vortex core that is observed. We note, however, that this does not change the domain wall width, as seen from our micromagnetic simulations of disks subjected to small magnetic fields.

The width of the domain wall is the result of the energetic compromise between the exchange, anisotropy and dipolar interaction terms: while close to the perimeter of the disk, the magnetization minimizes the free magnetic poles by remaining parallel to the perimeter, in the center of the disk, the spins try to orient along the magnetocrystalline easy axes. This results in a rather wide geometrically constrained domain wall, whose width decreases from the outside towards the center of the disk. The domain wall width δ as a function of the normalized distance from the center of the disk is shown in Fig. 5. (The experimental data suggest that the variation of the domain wall width scales with the distance between the vortex core and the disk radius.) For small distances from the vortex core the DW width assumes a value close to $(\pi/2)(A/K)^{1/2}$, while at the periphery of the disk it assumes a value close to the geometrical parameter $r_0\pi/2$ corresponding to a circular magnetization configuration. The situation in this case is analogous to the case of edge curling walls in patterned elements[25–27] and resembles also the equivalent in thick films of domain walls in closure

FIG. 5. Domain wall width as a function of the normalized distance from the vortex core.

domains,[28] where minimization of the magnetic energy is achieved by extended domain walls that may reach the periphery of the element or the surface of the film, respectively. The experimental values show the same trend as the calculations, a plateau followed by an upturn in the domain width with increasing distance from the vortex core, although the value of the domain wall at the plateau is a factor of 2 larger than that predicted by the simulations. This discrepancy may be either due to a smaller magnetocrystalline anisotropy constant than that measured in continuous films or due to a larger exchange constant than that assumed in the calculations (or a combination of these two factors).

In conclusion, we have studied the remanent magnetic configuration in fcc Co small disk elements. The prevalent state corresponds to a nearly closed flux, four-quadrant configuration typical of systems with cubic anisotropy. Less frequently, other magnetic states may be stabilized by pinning sites for the domain wall during the transition from saturation to remanence. We show how the shape of the element combined with the cubic anisotropy energy term determines not only the equilibrium domain structure (quadrant state), but also gives rise to a geometrically constrained domain wall whose width increases with the distance from the vortex core. Both the observed remanent states and the measured width of the domain wall agree well with micromagnetic calculations, showing, therefore, that the observed domain wall structure is characteristic of small elements where the magnetocrystalline anisotropy strength is significant as compared to the dipolar interaction.

*Corresponding author. E-mail address: jacb1@phy.cam.ac.uk

[1] J.-G. Zhu, Y. Zheng, and G.A. Prinz, J. Appl. Phys. **87**, 6668 (2000).

[2] J. Rothman, M. Kläui, L. Lopez-Diaz, C.A.F. Vaz, A. Bleloch, J.A.C. Bland, Z. Cui, and R. Speaks, Phys. Rev. Lett. **86**, 1098 (2001).

[3] Y. Zheng and J.-G. Zhu, J. Appl. Phys. **81**, 5471 (1997).

[4] R.P. Cowburn, D.K. Koltsov, A.O. Adeyeye, M.E. Welland, and D.M. Tricker, Phys. Rev. Lett. **83**, 1042 (1999).

[5] G. Gubbiotti, L. Albani, G. Carlotti, M.D. Crescenzi, E.D. Fabrizio, A. Gerardino, O. Donzelli, F. Nizzoli, H. Koo, and R.D. Gomez, J. Appl. Phys. **87**, 5633 (2000).

[6] T. Pokhil, D. Song, and J. Nowak, J. Appl. Phys. **87**, 6319 (2000).

[7] T. Okuno, K. Shigeto, T. Ono, K. Mibu, and T. Shinjo, J. Magn. Magn. Mater. **240**, 1 (2002).

[8] J.M. García, A. Thiaville, J. Miltat, K.J. Kirk, J.N. Chapman, and F. Alouges, Appl. Phys. Lett. **79**, 656 (2001).

[9] M. Kläui, J. Rothman, L. Lopez-Diaz, C.A.F. Vaz, J.A.C. Bland, and Z. Cui, Appl. Phys. Lett. **78**, 3268 (2001).

[10] L.D. Buda, I.L. Prejbeanu, M. Demand, U. Ebels, and K. Ounadjela, IEEE Trans. Magn. **37**, 2061 (2001).

[11] R. Pulwey, M. Zölfl, G. Bayreuther, and D. Weiss, J. Appl. Phys. **91**, 7995 (2002).

[12] C.A.F. Vaz, L. Lopez-Diaz, M. Kläui, J.A.C. Bland, T.L. Monchesky, J. Unguris, and Z. Cui, presented at the *46th Annual Conference on Magnetism and Magnetic Materials, Seattle, Washington, 2001* (unpublished).

[13] M. Kläui, C.A.F. Vaz, J. Rothman, J.A.C. Bland, W. Wernsdorfer, G. Faini, and E. Cambril, Phys. Rev. Lett. **90**, 097202 (2003).

[14] P. Bruno, Phys. Rev. Lett. **83**, 2425 (1999).

[15] S.P. Li, D. Peyrade, M. Natali, A. Lebib, Y. Chen, U. Ebels, L.D. Buda, and K. Ounadjela, Phys. Rev. Lett. **86**, 1102 (2001).

[16] C.A.F. Vaz and J.A.C. Bland, Phys. Rev. B **61**, 3098 (2000).

[17] R. Naik, C. Kota, J.S. Payson, and G.L. Dunifer, Phys. Rev. B **48**, 1008 (1993).

[18] M. Kowalewski, C.M. Schneider, and B. Heinrich, Phys. Rev. B **47**, 8748 (1993).

[19] B. Heinrich and J.F. Cochran, Adv. Phys. **42**, 523 (1993).

[20] B. Hillebrands, J. Fassbender, R. Jungblut, G. Guntherodt, D. Roberts, and G. Gehring, Phys. Rev. B **53**, R10548 (1996).

[21] M. Kläui, L. Lopez-Diaz, J. Rothman, C.A.F. Vaz, J.A.C. Bland, and Z. Cui, J. Magn. Magn. Mater. **240**, 7 (2002).

[22] M.R. Scheinfein, J. Unguris, M.H. Kelley, D.T. Pierce, and R.J. Celotta, Rev. Sci. Instrum. **61**, 2501 (1990).

[23] The Object Oriented MicroMagnetic Framework (OOMMF) project, ITL/NIST. See, http://math.nist.gov/oommf

[24] H. Fujiwara, H. Kadomatsu, and T. Tokunaga, J. Magn. Magn. Mater. **31−34**, 809 (1983).

[25] K. Yamamoto, H. Matsuyama, Y. Hamakawa, and M. Kitada, J. Appl. Phys. **75**, 2998 (1994).

[26] Y. Guo and J.-G. Zhu, J. Appl. Phys. **75**, 6388 (1994).

[27] R. Mattheis, K. Ramstöck, and J. McCord, IEEE Trans. Magn. **33**, 3993 (1997).

[28] A. Hubert and W. Rave, J. Magn. Magn. Mater. **196−197**, 325 (1999).